Manipulating light with photonic crystals

J. D. Joannopoulos
Department of Physics and Center for Materials Science and Engineering, Massachusetts Institute of Technology, Cambridge, MA 02139–4307, USA

ABSTRACT

Within the past several years we have witnessed the emergence of a new class of materials which provide capabilities along a new dimension for the control and manipulation of light. These materials, known as "photonic crystals," are viewed ideally as a composite of a periodic array of macroscopic dielectric scatterers in a homogeneous dielectric matrix. A photonic crystal affects the properties of a photon in much the same way that a semiconductor affects the properties of an electron. Consequently, photons in photonic crystals can have band structures, localized defect modes, surface modes, etc. This new ability to mold and guide light leads naturally to many novel applications of these materials in a variety of fields including optoelectronics, telecommunications, medicine and pharmaceuticals. An introductory survey including recent exciting developments in the field of photonic crystals is presented.

Keywords: Photonic crystals, optical waveguides, multilayer films, microcavities

1. INTRODUCTION

For the past 50 years, semiconductor physics has played a vital role in almost every aspect of modern technology. Advances in this field have allowed scientists to tailor the conducting properties of certain materials and have initiated the transistor revolution in electronics. New research suggests that we may now be able to tailor the properties of light. The key in achieving this goal lies in the use of a new class of materials called photonic crystals[1]. The underlying concept behind these materials stems from the pioneering work of Yablonovitch[2] and John[3]. The basic idea is to design materials that can affect the properties of photons in much the same way that ordinary semiconductor crystals affect the properties of electrons. This is achieved by constructing a crystal consisting of a periodic array of macroscopic uniform dielectric (or possibly metallic) "atoms." In this crystal, photons can be described in terms of a bandstructure, as in the case of electrons. Of particular interest is a photonic crystal whose bandstructure possesses a complete photonic band gap (PBG). A PBG defines a range of frequencies for which light is forbidden to exist inside the crystal. Forbidden, that is, unless there is a defect in the otherwise perfect crystal. A defect could lead to localized photonic states in the gap, whose shapes and properties would be dictated by the nature of the defect. Moreover, a very significant and attractive difference between photonic crystals and electronic semiconductor crystals is the former's inherent ability to provide complete tunability. A defect in a photonic crystal could, in principle, be designed to be of any size, shape or form and could be chosen to have any of a wide variety of dielectric constants. Thus, defect states in the gap could be tuned to any frequency and spatial extent of design interest. In addition to tuning the frequency, one also has control over the symmetry of the localized photonic state. All of these capabilities provide a new "dimension" in our ability to "mold" or control the properties of light. In this sense defects are *good* things in photonic crystals and therein lies the exciting potential of photonic crystals. Photonic crystals should allow us to manipulate light in ways that have not been possible before. The purpose of this paper is to highlight some of these novel possibilities.

Experimentalists have begun exploring the possibilities of fabricating such periodic structures with semiconductor-based, insulator-based, and metallodielectric-based materials at micrometer and submicrometer lengthscales. In this paper we shall introduce concepts and properties that are valid, in general, in three-dimensional photonic crystals, but for the sake of simplicity and ease of visualization most of our examples will involve two-dimensional photonic crystals. For definiteness, we consider a perfect array of infinitely long dielectric rods located on a square lattice of lattice constant a and investigate the propagation of light in the plane normal to the rods. The rods have a radius of $0.20a$, and a refractive index of 3.4 (which corresponds to GaAs at a wavelength of 1.55 micron). Such a structure possesses a complete gap between the first and the second transverse magnetic (TM) modes. (For TM modes, the electric field is parallel to the rods). Once we have a band gap, we can introduce a defect inside the crystal to trap or localize light. In particular, we shall investigate defects and defect-complexes that can correspond to specific components and devices such as waveguides, waveguide bends, microcavities, and

Optical Fibers and Sensors for Medical Applications, Israel Gannot, Editor,
Proceedings of SPIE Vol. 4253 (2001) © 2001 SPIE · 1605-7422/01/$15.00

channel-drop filters. Finally, we shall conclude this paper with a discussion of some novel and surprising properties that have been recently shown to be achievable using one-dimensionally periodic photonic crystals (i.e. traditional multilayer films).

2. PHOTONIC CRYSTAL WAVEGUIDES

By making a line defect, we can create an extended mode that can be used to guide light. Using photonic crystals to guide light constitutes a novel mechanism. Traditionally, wave-guiding is achieved in dielectric structures, such as optical fibers, by total internal reflection. When the fibers are bent very tightly, however, the angle of incidence becomes too large for total internal reflection to occur, and light escapes at the bend. Photonic crystals can be designed to continue to confine light even around tight corners.

To illustrate this point, we remove a row of dielectric rods from the photonic crystal described above. This has the effect of introducing a single guided-mode band inside the gap. The field associated with the guided mode is strongly confined in the vicinity of the defect and decays exponentially into the crystal. An intriguing aspect of photonic crystal waveguides is that they provide a unique way to guide optical light, tractably and efficiently, through narrow channels of air. Once light is introduced inside the waveguide, it really has nowhere else to go. The only source of loss is reflection from the waveguide input. This suggests that we may use photonic crystals to guide light around tight corners (Figure 1). Although the radius of curvature of the bend is less than the wavelength of the light, nearly all the light is transmitted through the bend over a wide range of frequencies through the gap. The small fraction of light that is not transmitted is reflected. For specific frequencies, 100% transmission can be achieved[4]. Note that a critical and necessary condition for 100% transmission efficiency is that the photonic crystal waveguide be *single-mode* in the frequency range of interest.

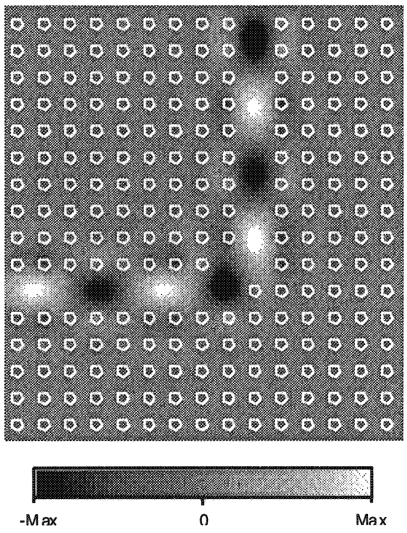

Figure 1: Electric field pattern in the vicinity of the sharp 90-degree bend. The electric field is polarized along the axis of the dielectric rods. The white circles indicate the position of the rods. Note that unlike the mechanism of total internal reflection, a photonic crystal may allow light to be guided in air.

A recent experimental verification of 100% transmission efficiency at very sharp bends is illustrated in Fig. 2. These are results from S. Y. Lin *et al.*[5] who performed experiments at microwave lengthscales for a series of waveguide bends (similar to the configuration in Fig. 1) using an appropriately scaled square lattice of alumina rods in air. The filled circles are experimental measurements and the open circles are the theoretical prediction. Good agreement is obtained over a wide range of frequencies.

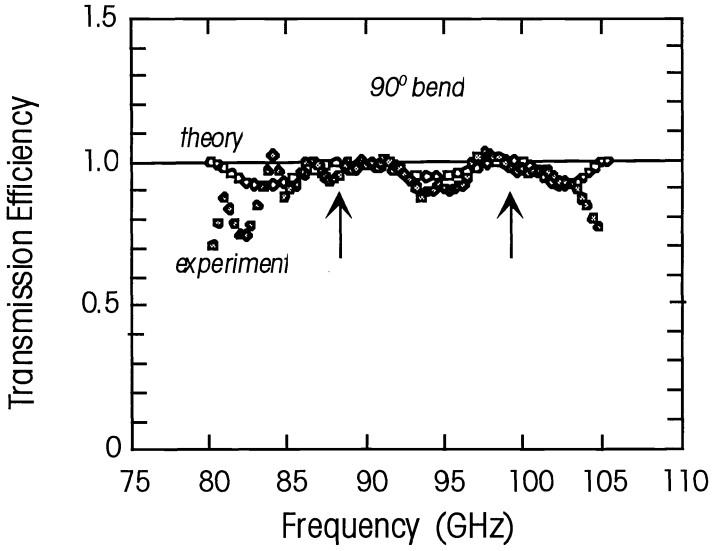

Figure 2: Transmission efficiency around a sharp 90-degree bend for a waveguide "carved out" of a square lattice of alumina rods in air. The filled circles are experimental measurements and the open circles are the theoretical prediction.

3. PHOTONIC CRYSTAL MICROCAVITIES

In addition to making line defects, we can also create local imperfections that trap light at a point within the crystal. As a simple example, let us choose a single rod and form a defect by changing its radius. Figure 3 shows the defect-state frequencies for several values of the defect radius. Let us begin with the perfect crystal — where every rod has a radius of $0.20a$ — and gradually reduce the radius of a single rod. Initially, the perturbation is too small to localize a state inside

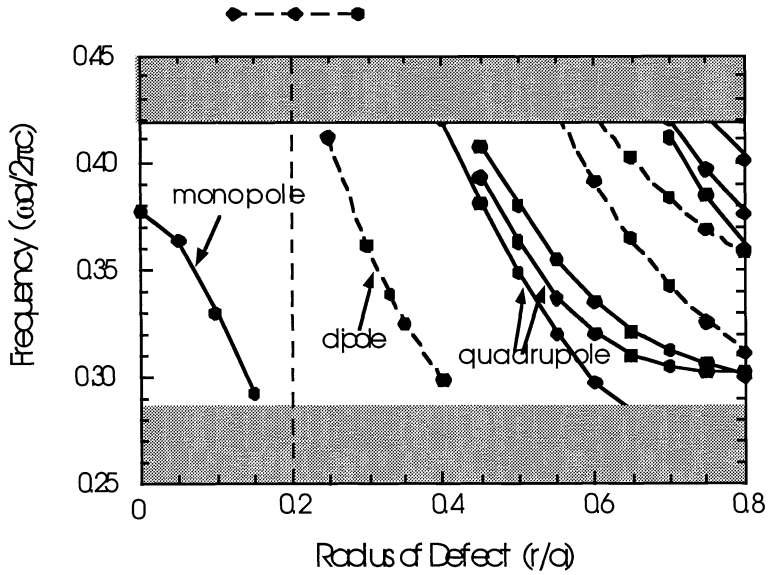

Figure 3: Defect states introduced into the gap by changing the radius of a single rod in an otherwise perfect square lattice of dielectric rods in air. When the radius is $0.2a$ there is no defect and when the radius is zero the rod has been completely removed. The shaded regions indicate the edges of the band gap.

the crystal. When the radius reaches $0.15a$, a singly-degenerate symmetric localized state appears in the vicinity of the defect. Since the defect involves removing dielectric material in the crystal, the state appears at a frequency close to the lower edge of the band gap. As the radius of the rod is further reduced, the frequency of the defect state sweeps upward across the gap.

Instead of reducing the size of a rod, we also could have made it larger. Starting again with a perfect crystal, we gradually increase the radius of a rod. When the radius reaches $0.25a$, two doubly-degenerate modes appear at the top of the gap. Since the defect involves adding material, the modes sweep downward across the gap as we increase the radius. They eventually disappear into the continuum (below the gap) when the radius becomes larger than $0.40a$. The electric fields of these modes have two nodes in the plane and are thus dipolar in symmetry. If we keep increasing the radius, a large number of localized modes can be created in the vicinity of the defect. Several modes appear at the top of the gap: first a quadrupole, then another (non-degenerate) quadrupole, followed by a second-order monopole and two doubly-degenerate hexapoles. We see that both the frequency and symmetry of the resonant mode can be tuned simply by adjusting the size of the rod. One important aspect of a finite-sized microcavity is its quality factor Q, defined as $\lambda/\delta\lambda$ where $\delta\lambda$ is the width of the cavity resonance. It is a measure of the optical energy stored in the microcavity over the cycle-average power radiated out of the cavity. P. Villeneuve *et al.*[6] have studied a finite-sized crystal made of dielectric rods where a single rod has been removed. They find that value of Q increases exponentially with the number of rods and reaches a value close to 10^4 with as little as four rods on either side of the defect. Also note that these cavities possess small modal volumes on the order of $(\lambda/2n)^3$. The combination of large quality factor with small modal volume offers a unique capability of maximally enhancing spontaneous emission.

4. CHANNEL DROP FILTERS

One of the most prominent devices in the telecommunications industry is the channel drop filter. This prominence is a consequence of both its importance and its size (~10cm×10cm)! Channel dropping filters are devices that are necessary for the manipulation of Wavelength Division Multiplexed (WDM) optical communications, whereby one channel is dropped at one carrier wavelength, leaving all other channels unaffected. Photonic crystals present a unique opportunity to investigate the possibilities of miniaturizing such a device to the scale of the wavelength of interest — 1.55 microns. We now combine line defects and point defects to make a novel photonic crystal channel-drop filter that gives access to one channel of a wavelength division multiplexed signal while leaving other channels undisturbed. Two parallel waveguides — a main transmission line and a secondary waveguide — are created inside a photonic crystal by removing two rows of dielectric rods. A resonant cavity is introduced between the two waveguides by creating one or more local defects. Resonant cavities are attractive candidates for channel dropping since they can be used to select a single channel with a very narrow linewidth. The performance of the filter is determined by the transfer efficiency between the two waveguides. Perfect efficiency corresponds to complete transfer of the selected channel — into either the forward or backward direction in the secondary waveguide — with no forward transmission or backward reflection in the main transmission line. All other channels should remain unaffected by the presence of the optical resonator. Fan *et al.*[7-8] have proved that there are three conditions that need to be satisfied by the coupling resonator in order to achieve optimal channel dropping performance:

(1) The resonator must possess at least two resonant modes, each of which must be even and odd, respectively, with regard to the mirror plane of symmetry perpendicular to the waveguides.

(2) The modes must be degenerate (or nearly so). Note that the intrinsic symmetry of the system does not support degeneracies, consequently one must force an accidental degeneracy!

(3) The modes must have an equal Q (or nearly so).

All three conditions are necessary in order to achieve complete transfer. The reflected amplitude in the transmission line originates solely from the decay of the localized states. The reflection therefore will not be cancelled if the optical resonator supports only a single mode. To ensure the cancellation of the reflected signal, the structure must possess a plane of mirror symmetry perpendicular to both waveguides, and support two localized states with different symmetry with respect to the mirror plane, one even and one odd. Since the states have different symmetries, tunneling through each one constitutes an independent process. The even state decays with the same phase along both the forward and backward directions while the odd state decays with opposite phase. When the two tunneling processes are combined, because of the phase difference, the decaying amplitudes cancel along the backward direction of the transmission line. In order for cancellation to occur, the lineshapes of the two resonances must overlap. Since each resonance possesses a Lorentzian lineshape, both resonances must

have substantially the same center frequency and the same width. When such degeneracy occurs, the incoming wave interferes destructively with the decaying amplitude along the forward direction in the transmission line, leaving all the power to be transferred into the secondary waveguide at the resonant frequency.

A photonic crystal system provides precisely the control necessary in order to satisfy all three conditions. An example of a photonic crystal channel-drop filter is shown in Figure 4. The cavity consists of a single point defect with a radius $0.60a$.

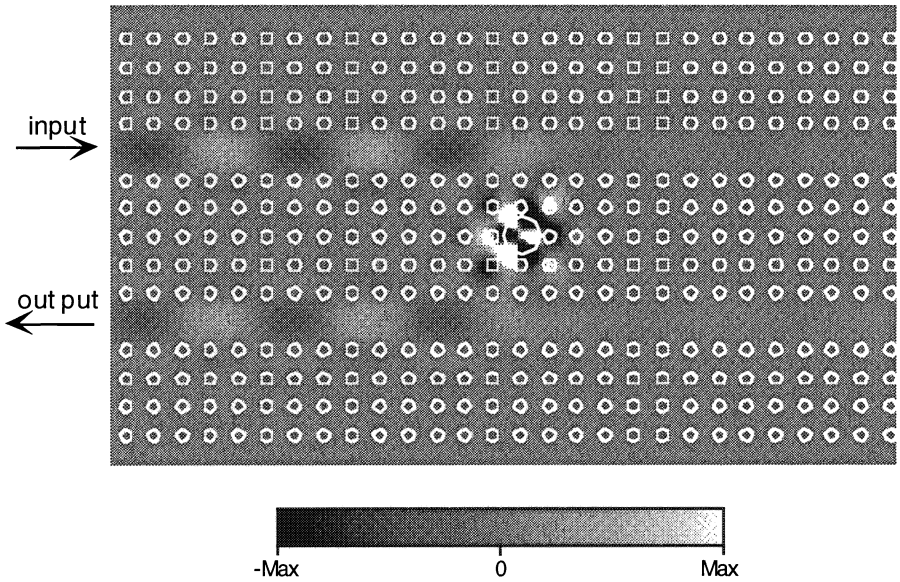

Figure 4: Steady-state field distribution of the photonic crystal channel drop filter at resonance. Note that the size of this device is on the order of the wavelength of the light in air.

As we have already seen (Figure 3) this defect supports a doubly-degenerate hexapole state near $\omega_0 = 0.39\ (2\pi c/a)$ with the required symmetry. However, the presence of the waveguides next to the cavity breaks the degeneracy of the hexapoles. To restore the degeneracy, we change the dielectric constant (or equivalently the size) of two rods adjacent to the defect. By properly changing the rods, we can affect the modes in different ways and force an accidental degeneracy in frequency. An approximate degeneracy in width exists between the states since the hexapoles possess large enough orbital angular momentum to ensure roughly equal decay of the even and odd modes into the waveguides. We simulate the filter response of the structure by sending a pulse through the upper waveguide. The transmission in the main line is close to 100% for every channel, except at the resonant frequency, where the transmission drops to 0% and the transfer efficiency approaches 100%. The quality factor is larger than 6,000. Since the even state (even with respect to the mirror plane perpendicular to the waveguides) is odd with respect to the mirror plane parallel to the waveguides, the transfer occurs along the backward direction in the secondary waveguide. Finally, although the lineshape of the current resonant modes is Lorentzian, it can be modified to be of the preferred "square-wave" shape by introducing complexes of coupled resonant modes as discussed in detail in Ref. 9.

5. MULTILAYER FILMS

As we have seen a photonic crystal can be a perfect mirror of light from any direction, with any polarization, within a specified frequency range. It is natural to assume that a necessary condition for such omnidirectional reflection is that the crystal exhibit a complete three-dimensional photonic bandgap. Recently, it has been shown[10-12] that this assumption is false - in fact a one-dimensional photonic crystal or dielectric multilayer film will suffice!

A one-dimensional photonic crystal has an index of refraction that is periodic in the y coordinate and consists of an endlessly repeating stack of dielectric slabs, which alternate in thickness from d_1 to d_2 and an index of refraction from n_1 to n_2. Incident light can be either s polarized (**E** is perpendicular to the plane of incidence) or p polarized (parallel). Because the medium is periodic in y and homogeneous in x and z, the electromagnetic modes can be characterized by a wave vector **k**, with k_y

restricted to $0 \leq k_y \leq \pi/a$. We may suppose that $k_z = 0$, $k_x \geq 0$, and $n_2 > n_1$ without loss of generality. The allowed mode frequencies ω_n for each choice of $\mathbf{k}$ constitute the band structure of the crystal. The continuous functions $\omega_n(\mathbf{k})$, for each n, are the photonic bands.

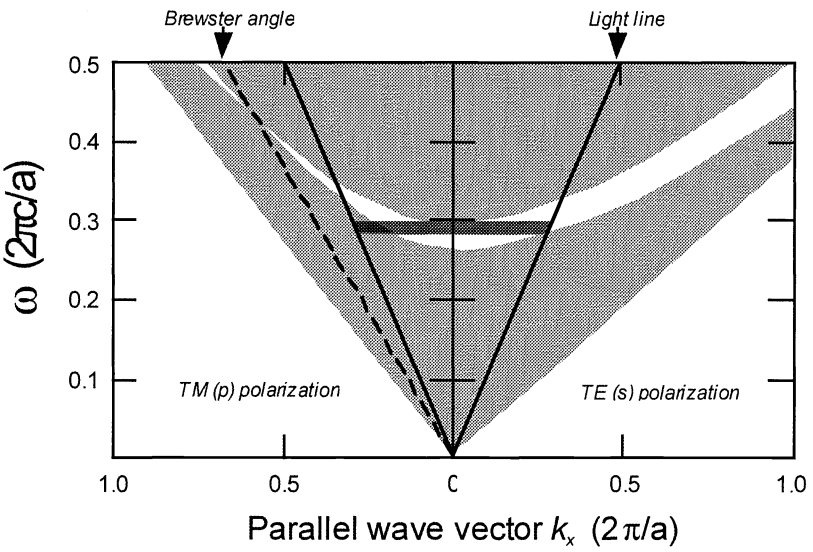

Figure 5: Projected bandstructure for a multilayer film that is *not* omnidirectionally reflecting.

For an arbitrary direction of propagation, it is convenient to examine the projected band structure (Figure 5) for a quarter-wave stack with $n_1 = 1.7$ and $n_2 = 2.2$. To make this plot we first computed the bands $\omega_n(k_x,k_y)$ for the structure, using a numerical method to solve Maxwell's equations in a periodic medium. (In fact, for the special case of a multi-layer film, an analytic expression for the dispersion relation is available.) Then, for each value of k_x, the mode of frequencies ω_n for all possible values of k_y were plotted. Thus in the light gray regions there are electromagnetic modes for some value of k_y, whereas in the white regions there are no electromagnetic modes, regardless of k_y.

One obvious feature in this figure is that there is no complete bandgap. For any frequency there exists some electromagnetic mode with that frequency - the normal-incidence bandgap is crossed by modes with $k_x > 0$. This is a general feature of one-dimensional photonic crystals. However, the absence of a complete bandgap does not preclude omnidirectional reflection. The criterion is not that there be no propagating states within the crystal; rather, the criterion is that there be no propagating states that can couple to an incident propagating wave. As we argue below, the latter criterion is equivalent to the existence of a frequency range in which the projected band structures of the crystal and the ambient medium have no overlap.

The electromagnetic modes in the ambient medium obey $\omega = c(k_x^2 + k_y^2)^{1/2}$, where c is the speed of light in the ambient medium, so generally $\omega > ck_x$. The whole region above the solid diagonal light lines $\omega = ck_x$ is filled with the projected bands of the ambient medium. If a semi-infinite crystal occupies $y < 0$ and the ambient medium occupies $y > 0$, the system is no longer periodic in the y direction and the electromagnetic modes of the system can no longer be classified by a single value of k_y. These modes must be written as a weighted sum of plane waves with all possible k_y. However, k_x is still a valid symmetry label. The angle of incidence θ upon the interface at $y = 0$ is related to k_x by $\omega \sin\theta = ck_x$.

For there to be any transmission through the semi-infinite crystal at a particular frequency, there must be an electromagnetic mode available at that frequency that is extended for both $y > 0$ and $y < 0$. Such a mode must be present in the projected photonic band structures of both the crystal and the ambient medium. (The only states that could be present in the semi-infinite system that were not present in the bulk system are surface states, which decay exponentially in both directions away from the surface and are therefore irrelevant to the transmission of an external wave). Therefore, the criterion for omnidirectional reflection is that there exist a frequency zone in which the projected bands of the crystal have no states with $\omega > ck_x$..

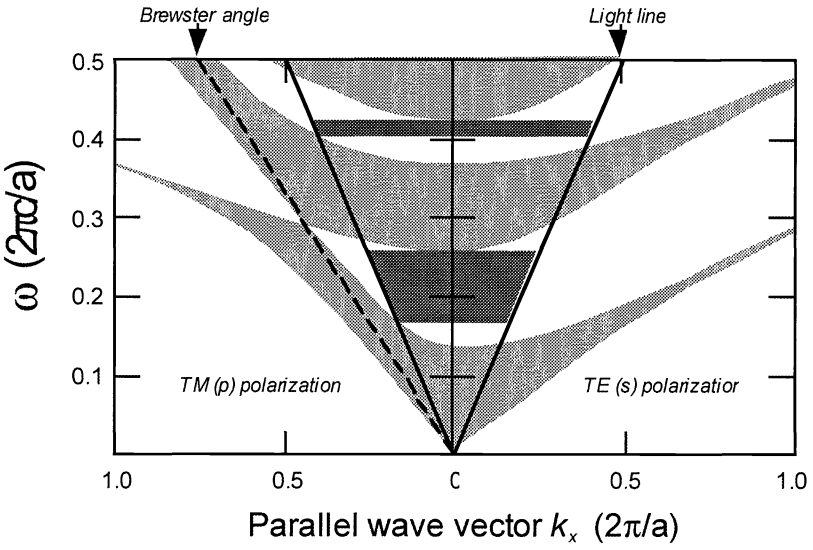

Figure 6: Projected bandstructure for a multilayer film that *is* omnidirectionally reflecting.

This difficulty vanishes when we lower the bands of the crystal relative to those of the ambient medium by raising the indices of refraction of the dielectric films. Figure 6 shows the projected band structure for the case $n_1 = 1.6$ and $n_2 = 4.6$. In this case there is a frequency zone in which the projected bands of the crystal and ambient medium do not overlap, namely, the dark gray regions. This zone is bounded above by the normal-incidence bandgap and below by the intersection of the top of the first light gray region for *p*-polarized waves with the light line. For any frequency lying within the dark gray regions there will be total reflection from any incident angle for either polarization!

6. THE OMNIGUIDE

The recent emergence of a dielectric omnidirectional multilayer structure as described above opens new opportunities for low loss broadband guiding of light in air. Light guided in a hollow waveguide lined with an omnidirectional reflecting film will propagate primarily through air and will therefore have substantially lower absorption losses.[13] In addition, the confinement mechanism is not angular dependant and this allows the light to be guided around sharp bends with little or no leakage. A cross section of a hollow tube waveguide is shown schematically in Figure 7. Conceptually, hollow waveguides constructed

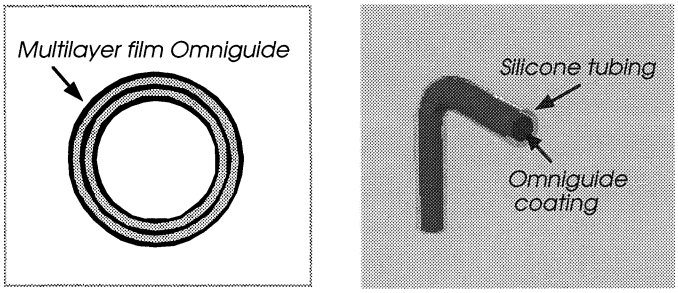

Figure 7: Schematic representation of an Omniguide hollow dielectric waveguide.

out of multilayer films were first studied in the late 70's.[14] The important difference here is the use of an omnidirectional reflecting multilayer structure. This is crucial in order to ensure confinement over all frequencies contained in the omnidirectional range.

As a demonstration of the effectiveness of such an approach a Te/polymer broad band, low loss hollow waveguide in the 10 micron regime was fabricated and its transmission measured around a 90^0 bend.[13] The generality of the solution enables the application of the method to many important wavelengths of interest, including telecommunication applications, as well as high power laser guiding in medical and other fields of use. The details of fabrication and measurement are as follows:

A Drummond 1.92mm o.d. silica glass capillary tube was cleaned in concentrated sulfuric acid. The first Te layer was thermally evaporated using a LADD 30000 evaporator fitted with a Sycon Instruments STM100 film thickness monitor. The capillary tube was axially rotated to ensure uniformity during coating. The first polymer layer was deposited by dip coating the capillary tube in a solution of 5.7g polystyrene DOW 615APR in 90g toluene. The next layer of Te was deposited in the same method outlined above. The subsequent polymer layers were made of polyurethane diluted in mineral spirits. The resulting guide has a total of 9 layers; 5 Te and 4 polymer and a total length of 10cm. The layer thicknesses are approximately 0.8μm for the tellurium layer (refractive index 4.6) and 1.6μm for the polystyrene layer (refractive index 1.59). The coated capillary tube was then inserted in a heat shrink tube filled with silicone rubber. Finally, the glass tube was dissolved using concentrated hydrofluoric acid (48%). The resulting hollow tube assembly is thus lined with the mirror coating and is both flexible and mechanically stable.

Transmission measurements (using a Nicolet Magna 860 FTIR bench with an MCT/A detector) were performed around a 90^0 bend at a radius of curvature of about 1cm and were normalized to a straight tube measurement (Figure 8). The results are

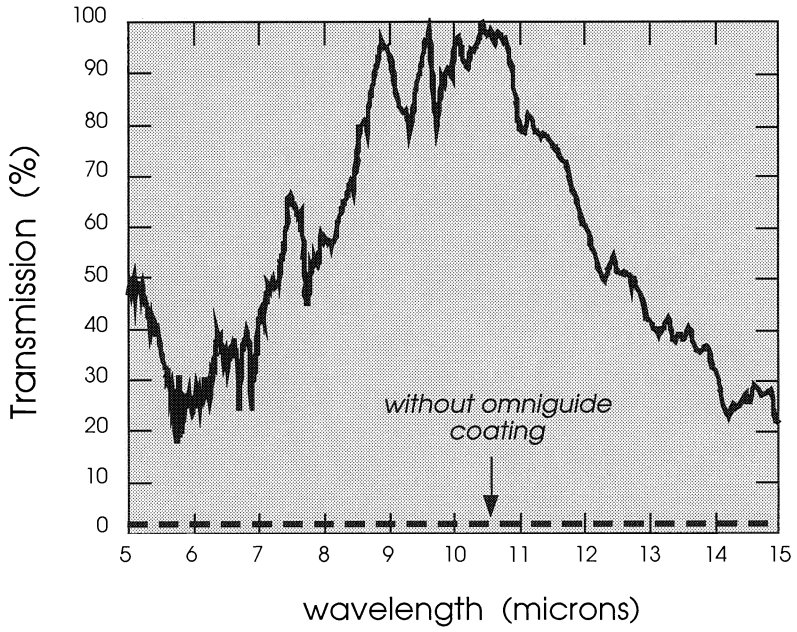

Figure 8: Transmission through a 90 degree bend in a hollow tube omniguide.

quite striking and indicate a high transmission around the 90^0 bend for a spectral band that corresponds nicely to the omnidirectional reflectivity range of about 8 to 12μm. The relatively high noise level is due to lack of purge. Finally, although our proof of concept demonstration involves a large diameter multimode waveguide, one could fabricate a much smaller tube that could in principle be made to support a single mode. Work to accomplish this is currently underway.

7. PHOTOACTIVATED DRUG THERAPY

A preponderance of the current therapeutic treatment methods involves *systemic* administration of drugs for treatment of *local* disorders. This inherent characteristic of conventional drug delivery is a major cause of side effects, lowers the treatment success rate, and leads to increased treatment costs. The importance of controlled in-vivo delivery of therapeutic agents has, of course, been realized for some time and is the subject of intensive research efforts in the US and abroad. The majority of studies and devices that exist to date involve methods for temporal controlled release – also known as sustained release. A number of other approaches have been explored in order to achieve localized drug delivery to non superficial locations. These include ultrasonic transducers, phased array antennas (to provide local heating in deep body locations), and microchip drug delivery. Recently, the work of Mitragotri et al.[15] describes an ultrasound-mediated transdermal delivery system that offers temporal and spatial control. While all of these approaches represent significant and useful contributions in the field of drug delivery, there still remains the need for low-cost, safe techniques for high-resolution spatially-controlled release of pharmaceuticals within a patient. Very recently, a novel drug delivery platform has been suggested[16] to overcome this limitation. In this proposal, by utilizing a novel biocompatible optical microcavity design, an efficient dissipation of electromagnetic energy in a very small volume could be achieved which then leads to the drug release. The controlled release mechanism is actuated by low intensity electromagnetic radiation in the near visible (0.65-1.3μm) spectrum (where absorption losses in water and red blood cells are low) and offers a high degree of temporal spatial and angular control of the release characteristics. In essence, the release mechanism is based on the creation of a high efficiency photon scavenging micro-container that dissipates most of the incident EM radiation energy in a very small volume thereby inducing a temperature change. By illuminating the structure with light of a particular frequency local heating occurs, the diffusion properties of the material change, and the therapeutic agent is released. A schematic of the

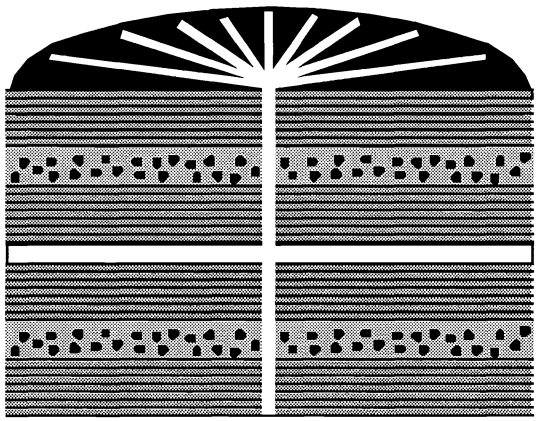

Figure 9: Schematic cross section of the photonic crystal controlled release micro-container. The light-gray micro-slabs contain the active binding material and therapeutic agent (black dots). The white regions represent soluble buffer material.

micro-container (size on the order of microns)is illustrated in Figure 9. It consists of photonic crystal regions (horizontal parallel lines) which in the simplest case can be omnidirectionally reflecting multilayer films. These regions sandwich the micro-cavity regimes (light gray micro-slabs). The micro-cavities are filled with a light absorbing material (absorber), with a material that changes its diffusion properties upon heating (gate), and with the therapeutic agent (black dots). Activation of the micro-cavities could proceed as follows. Two or more low intensity laser sources, with frequencies at the operating micro-cavity frequency, are focussed at a particular point in the body. The intersection of these laser beams defines an activation volume (thereby avoiding release of the drug along the pathway of the beams). As the micro-cavities pass through the blood stream they are only activated at this intersection. The energy concentrated in the micro-cavity regime is dissipated through absorption causing an increase in the micro-slab temperature, leading to a change in its diffusion properties (e.g. undergoes a phase transition or goes through a glass transition), which in turn results in the release of the therapeutic agent.

Finally, there are a number of possible methods for removing the unreleased portion of the drug. One approach could involve the metabolism of the optical confinement structure (i.e. the photonic crystal) which could be made of materials that can be

metabolized. The system would then break into smaller pieces and be removed by the kidneys. To facilitate this process, the system could be patterned during fabrication to contain regions that are biodegradable (white regions in Figure 9), that do not contain the drug but serve to buffer the smaller drug containing regions. After the periodic structure dissolves, the soluble regimes are exposed to the blood stream and are dissolved, leaving much smaller insoluble drug containing particles that can be removed by virtue of their small size.

All of this design is, of course, only at a very preliminary and conceptual stage at the moment, and many practical issues remain to be resolved and demonstrated. Nevertheless, we believe it offers a novel and intriguing direction for future research in the field of controlled spatial and temporal drug release.

ACKNOWLEDGEMENTS

The work described in this review was performed by Mihai Ibanescu, Joshua Winn, Dr. Attila Mekis, Dr. Shanhui Fan, Prof. Yoel Fink, and Prof. Edwin Thomas. This work is supported in part by the MRSEC program of the NSF under award number DMR-9400334.

REFERENCES

1. J. D. Joannopoulos, R. D. Meade, and J. N. Winn, *Photonic Crystals* (Princeton, New York, 1995).
2. E. Yablonovitch, *Phys. Rev. Lett.* **58**, 2509 (1987).
3. S. John, *Phys. Rev. Lett.* **58**, 2486 (1987).
4. A. Mekis, J. C. Chen, I. Kurland, S. Fan, P. R. Villeneuve, and J. D. Joannopoulos, *Phys. Rev. Lett.* **77**, 3787 (1996).
5. S. Y. Lin, E. Chow, V. Hietch, P. R. Villeneuve, and J. D. Joannopoulos, *Science* **282**, 274 (1998).
6. P. R. Villeneuve, S. Fan, and J. D. Joannopoulos, *Phys. Rev. B* **54**, 7837 (1996).
7. S. Fan, P. R. Villeneuve, J. D. Joannopoulos, and H. A. Haus, *Phys. Rev. Lett.* **80**, 960 (1998).
8. S. Fan, P. R. Villeneuve, J. D. Joannopoulos, and H. A. Haus, *Opt. Express* **3**, 4 (1998).
9. S. Fan, P. R. Villeneuve, J. D. Joannopoulos, M. J. Khan, C. Manolatou, and H. A. Haus, *Phys. Rev. B* **59**, 15882 (1999).
10. J. N. Winn, Y. Fink, S. Fan, and J. D. Joannopoulos, *Optics Letters* **23**, 1573 (1998).
11. Y. Fink, J. N. Winn, S. Fan, C. Chen, J. Michel, J. D. Joannopoulos, and E. L. Thomas, *Science* **282**, 1679 (1998).
12. D. Chigrin, A. Lavvrinenko, D. Yarotsky, and S. Gaponenko, *Appl.Phys.A* **68**, 25 (1999).
13. Y. Fink, D. J. Ripin, S. Fan, C. Chen, J. D. Joannopoulos, and E. L. Thomas, *J. Lightwave Tech.* **17**, 2039 (1999).
14. P. Yeh, A. Yariv, E. Marom, *J. Opt. Soc. Am.*, **68**, 9 (1978).
15. S. Mitrgotri, D. Blankschtein, and R. Langer, *Science* **269**, 850 (1995).
16. Y. Fink, E. L. Thomas, J. D. Joannopoulos, and J. W. Winkelman, unpublished (2000).